CHAPTER 2
INSTRUMENTS

The investigation in this thesis required observations from space-borne instruments in order to study X-ray emission in solar flares. Observations from ground-based instruments are used to study the geomagnetic activity. This chapter presents the details of space-borne instruments and ground-based instruments used for the study of solar and geomagnetic activity respectively.

A: Space-borne Instruments:

2.1 SOXS:

Solar X-ray Spectrometer (SOXS) is the first space-borne solar astronomy experiment of India. The “Solar X-ray Spectrometer (SOXS)” mission (Jain *et al.*, 2000a) was successfully launched onboard an Indian geostationary satellite namely GSAT-2 on 8 May 2003 by GSLV-D2 rocket. The SOXS aims to study the high spectral and temporal resolution X-ray spectra from solar flares. The SOXS consists of two independent payloads, viz. SOXS Low-Energy Detector (SLD) and SOXS High-Energy Detector (SHD) payloads. The SLD is comprised of two semiconductor devices, viz. silicon PIN detector for 4–25 keV (area 11.56 mm^2); and cadmium–zinc–telluride (CZT) detector for 4–56 keV energy range (area 25 mm^2). These state-of-the-art solid state detectors in SLD have superb sub-keV energy resolution and 100 ms temporal resolution characteristics, which make them most appropriate for solar flare research in the context of energy transport and acceleration time scales of particles. This section presents the details of the SLD instrumentation and its in-orbit performance. For my investigation I have employed observations from the SLD payload and the observations and results are discussed in Chapter 4.

The SLD payload consists of four subsystems, viz. SOXS Low Energy Detector (SLED) package; SOXS Sun Tracking Mechanism (SSTM), SOXS Low Energy Processing Electronics (SLE) package; and SOXS Common

Electronics (SCE) package. The SLD payload, spacecraft and mission characteristics are presented in Table 2.1 while the block scheme of the SLD payload is shown in Figure 2.1. I describe below the specifications and operations of various packages of the payload.

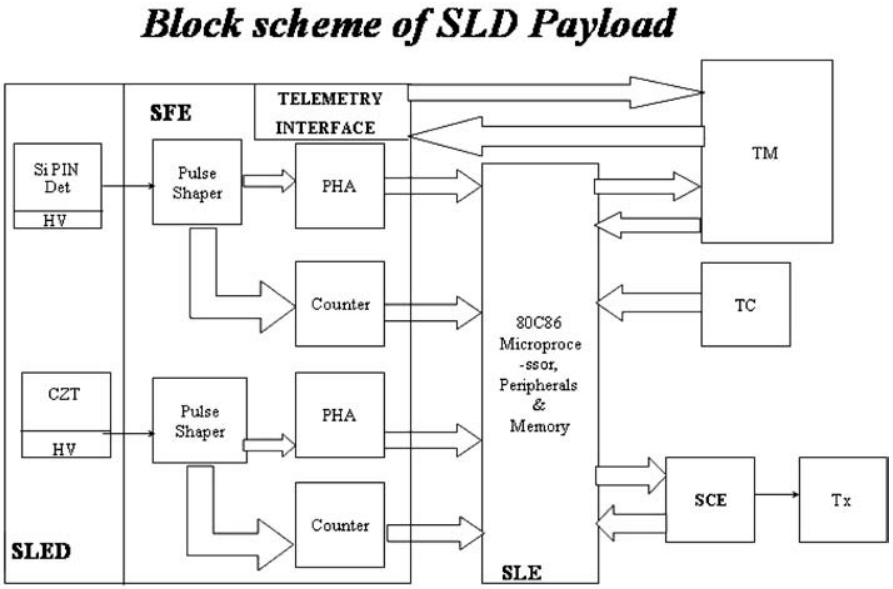

Figure 2.1: The block scheme of the SLD payload.

2.1.1 The Solid-state Detectors:

The state-of-the-art solid state detectors viz. Si PIN and CZT detectors (diodes) have been used, for the first time, for a dedicated space-borne solar astronomy experiment. These are new high performance X-ray detectors having a charge sensitive preamplifier and thermoelectric cooler system. The FET and the feedback circuit are also mounted on the cooler. These components are kept approximately at −20°C, and can be monitored by an internal temperature sensor. The detectors were developed at the Physical Research Laboratory using the hermetic TO-8 package from Amptek, USA. Special features of these detectors, which have been exploited to full potentiality to achieve the science goals, are shown in Table 2.2. In Table 2.3 specifications and operating conditions of CZT and Si detectors are presented.

Table 2.1 (SLD Characteristics)

1a. Instrument characteristics:		
Detectors:	Si PIN	CZT
Energy range:	4 - 25 keV	4 - 60 keV
Energy resolution (FWHM):	~700 eV at 5.9 keV, ~ 900 eV at 22.2 keV.	~1.5 keV at 5.9 keV ~1.8 keV at 22.2 keV
Temporal Resolution:		
Flare	100 ms	100 ms
Quiet	1 s temporal, 3 s spectral	1 s temporal, 3 s spectral
Field of view	full Sun (~3.4°)	full Sun (~3.4°)
Effective area:	~10^{-4} cm^2 at 4 keV ~10^{-2} cm^2 at 10 keV	~10^{-4} cm^2 at 4 keV ~10^{-1} cm^2 at 30 keV
Aspect system:	SOXS Sun Tracking Mechanism; Sun centered to <0.2°	
Mass:	18 kg	
Power:	20 watts	
Telemetry:	8 kbps, downlink	
On-board storage:	5 MB	
1b. Spacecraft characteristics:		
Payload:	SLD/SOXS, payload of opportunity	
Spacecraft:	GSAT-2, communication satellite	
Orbit:	Geostationary	
Altitude:	36400 km	
Nominal mission lifetime:	5 years	
1c. Mission characteristics:		
Launch Date:	8 May 2003	
Launch vehicle:	GSLV-D2	

Table 2.2

Special Features of the Detectors

- Si-PIN and CZT photodiode detectors
- Thermoelectric cooler (Peltier cooler)
- Cooled FET
- Temperature monitor
- Beryllium window
- Charge sensitive preamp
- Hermetic package (TO-8)
- Wide detection range
- Operation at near room temperature.

Various investigators have carried out the design, development and characterization of various kinds of Si and CZT detectors. Huber, Pantazis, and Jordanov (1995), Jordanov, Pantazis, and Huber (1996), and Desai, Pantazis, and Shah (1995) studied the response of high performance, thermoelectrically cooled X-ray and gamma ray detectors. They used compact Si and CZT detectors to explore their potentiality for high-resolution X-ray and gamma ray spectroscopy for future missions. The system used by them consists of a small cylindrical hybrid circuit including detector, FET and feedback components mounted on a small thermoelectric cooler. Huber, Pantazis, and Jordanov (1995) achieved energy resolution (FWHM) ~250 and 350 eV at 5.9 keV for Si PIN and CZT detectors respectively under all ideal conditions and at operating temperature of −20°C. Later, a detailed response study of CZT detectors to explore them as future spectroscopic detectors for X-ray astronomy was undertaken in a big way by several investigators over the globe (Jordanov, Pantazis, and Huber, 1996; Tousignant *et al*., 1997; Matteson *et al*., 1997; Kraft *et al*., 1998; Narita *et al*., 1997; Kuvvetli *et al*., 1999; Lachish, 1999, 2001).

A detailed design and development study on the application of XR-100CR (Si PIN) and XR-100T-CZT (CZT) detectors from Amptek, USA for the proposed

SLD payload was carried out by Jain *et al*. (2000b). A prototype model of the detector package was designed and developed at PRL, and thereafter characterization of the detectors was successfully carried out by Jain *et al*. (2002a). Later, the flight model was fabricated at Space Application Centre (SAC) of Indian Space Research Organisation (ISRO), Ahmedabad, India and pre-flight characterization was done by Jain *et al.* (2003) at Dr. Satish Dhawan Space Launching Facility, of ISRO at Shriharikota, India almost 2 weeks before the launch.

2.1.1.1 Collimator and Filter:

Si and CZT detectors have 0.025 and 0.250 mm thick Beryllium (Be) window to cut the background noise. However, in view of the application of these detectors for studying the Sun from a geostationary platform the thickness of Be window is not sufficient to cut the background significantly so as to achieve the S/N ratio >10. In this view a collimator and filter/attenuator were designed and fabricated at PRL.

The collimator is built of a 1.8 mm thick nickel sandwiched between 1.8 and 3.4 mm thick aluminum tubes. The length of the collimator is 56 and 81.5 mm for Si and CZT detectors respectively in order to achieve 3.4° FOV. In Figure 2.2 the SLED package is shown mounted on the aspect system viz. SOXS Sun Tracking Mechanism (SSTM). A 0.080 mm thick aluminum filter plus 0.15 mm thick kapton polyamide film are mounted on the Be window of the detector.

The Be window plus the aluminum and kapton films are good enough to eliminate the X-rays below 4 keV (solar and cosmic) and electrons and protons up to 300 keV and 2 MeV respectively that fall directly in the line of sight of the FOV. This enabled us to achieve S/N ratio ~100 in Si and ~50 in CZT. However, due to the 2 mm thick CZT substrate higher noise counts are observed as a function of energy.

Table 2.3

Specifications and Operating Conditions of SLED

Characteristics	**CZT**	**Si PIN**
Material doped	Cadmium-Telluride crystal doped with zinc	N type silicon wafer with P type material
Size	5 x 5 x 2 mm	3.6 x 3.6 x 0.3 mm
Be window thickness	0.25 mm	0.025 mm
Energy Resolution	1.2 keV at 5.9 keV	500 eV at 5.9 keV
Dark counts	$< 5 \times 10^{-3}$ cts/s at 10 keV < E < 1 MeV	$<3 \times 10^{-3}$ cts/s at 2 keV < E < 150 keV
Preamps	Amptek model A250 with current divider	Amptek model A250 with current divider
Operating Voltage	300 - 400 volts DC	100 volts DC
Temp. Monitor Sensor	1 μA/°K	1 μA/°K
Operating Temperature	-30 °C to -10 °C	-30 °C to -10 °C
Sensitivity	0.73 mV/keV	1 mV/keV
Pedigree	never flown in space	flown on Mars Pathfinder
Pre-Amps Power	± 8 volts at 25 mA	± 8 volts at 25 mA
Detector Power	+ 400 volts at 1μA	+100 volts at 1 μA
Cooler Power	2.1 volts at 0.7A	2.1 volts at 0.7A
Total Power	< 1 watt	< 1 watt

Shown in Figure 2.3 (left and right) are the effective area for Si PIN and CZT detectors folded over the efficiency of the detector and considering the above design for filter. It may be noted that almost no contribution arrives from X-rays below 4 keV where the Sun remains bright even outside of flare conditions. The design details of collimator and filter may be found in Jain *et al.* (2002b).

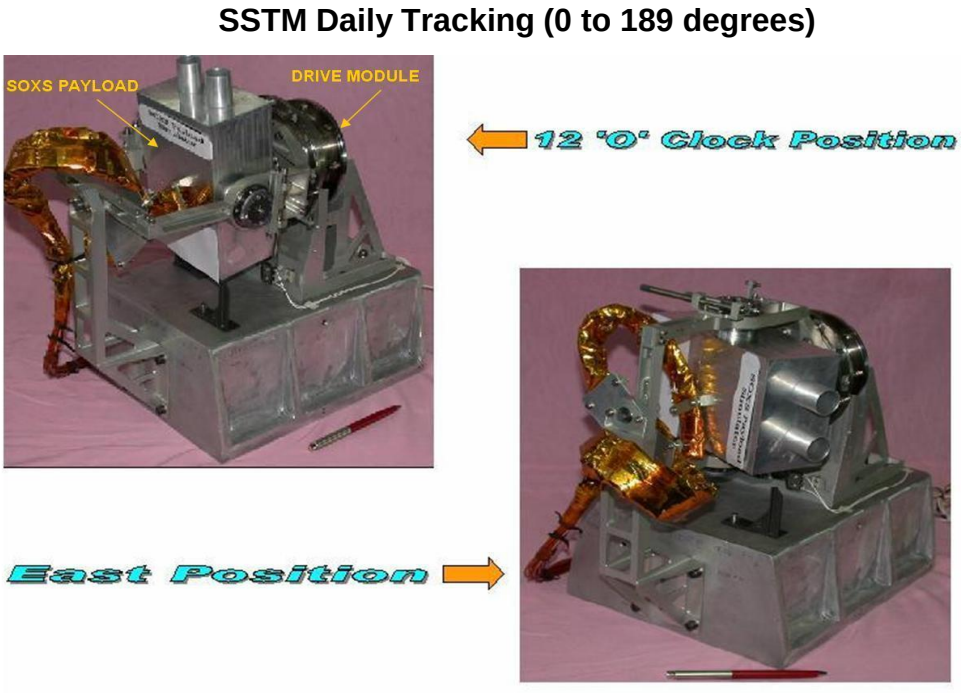

Figure 2.2: The detector package (see text) mounted on the SOXS Sun tracking mechanism (SSTM). The collimators are seen projecting outside. The FOV is 3.4°. The detector package moves in the line of sight of the Sun within an accuracy of about 0.1°. The SSTM has only one drive motor for correction in right ascension and declination.

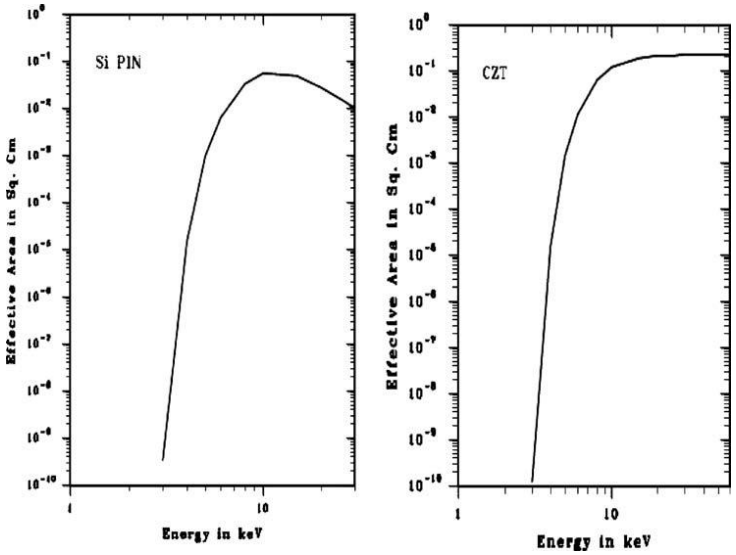

Figure 2.3: The effective area of the Si and CZT detectors of the SLED package. The Si and CZT have 0.025 and 0.25 mm Be windows respectively in front of the detector heads. Additional filters were mounted on the head to reject the background significantly.

2.1.1.2 Onboard Radioactive Source:

SLD carries a small onboard radioactive source namely Cd^{109} (5 microcuries, half life time 412 days) that emits lines at 22.2 and 25 keV, far from any line expected to occur in flare or in the detector's dynamic range by any varying background. The source is mounted on a M5 screw, which is inserted inside the collimator at an angle so as to direct the radiation on the center of the detector. The intensity of the source is further attenuated by 2 mm thick aluminum shield on the top of the source so that it forms the spectral lines after accumulating the counts over an hour or more. The 22.2 keV line is used for in-flight calibration of the Si detector by accumulating the counts for an hour. The calibration is conducted in night time as well as in the day time in the line of sight of the Sun. Similarly, for in-flight calibration of CZT detector, the 25 keV line in addition to the 22.2 keV line is used. The 22.2 keV line from the radioactive source and the 6.7 keV line from Fe XXVI emission during solar flares enable to monitor any energy band shift over the dynamic range of the detector as well as the FWHM as a function of the period elapsed from the launch.

In Figure 2.4 the results of in-flight calibration taken on 05 June 2003 during spacecraft nighttime for Si and CZT detectors are shown. It may be

noted that Si detector shows unambiguously 22.2 keV line arising from in-built Cd^{109} radioactive source irrespective to TEC ON or OFF condition. However, in the case of CZT we find shift of 14 channels as soon as we turn ON the TEC. This anomaly is due to grounding scheme adopted by us for CZT detector, and thereby it reveals both lines from Cd^{109} radioactive source at 22.2 keV and 25 keV shifted to 14 channels. In this view the dynamic energy range for CZT detector is now 4 keV to 56 keV instead of 4 keV to 60 keV.

2.1.2 SUN ASPECT SYSTEM – SOXS SUN TRACKING MECHANISM (SSTM):

The GSAT-2 is a communication satellite and SOXS is a payload of opportunity. The SLD payload is mounted on the anti-earth view (AEV) side of the spacecraft enabling the payload to look at the sky. However considering the limited FOV of 3.4°, an aspect system *viz*. SOXS Sun Tracking Mechanism (SSTM) was designed and developed at Spacecraft Mechanisms Group of ISRO Satellite Centre. The SSTM is unique in terms that it employs only a single drive module and keeps the Sun tracking in both right ascension and declination (Viswanatha, 2000). The SSTM consists of one stepper motor drive module with a gear reducer, and attached to it is a frame with the Declination Tilt Mechanism above which the detector package (SLED) is mounted. The drive module (Figure 2.2) consists of a stepper motor and a pancake type harmonic drive gear reducer. The stepper motor is a two-piece motor, and Duplex pair of angular contract ball bearings fixes on the motor to the input shaft. The motor drives the input shaft in steps of 1°. The input shaft drives the harmonic drive. The fixed gear of the harmonic drive is fixed to the outer housing and the rotating dynamic gear is mounted on a four-point contact ball bearing and the output flange is fixed on the outer side. The gear reducer has 1:157 gear reduction.

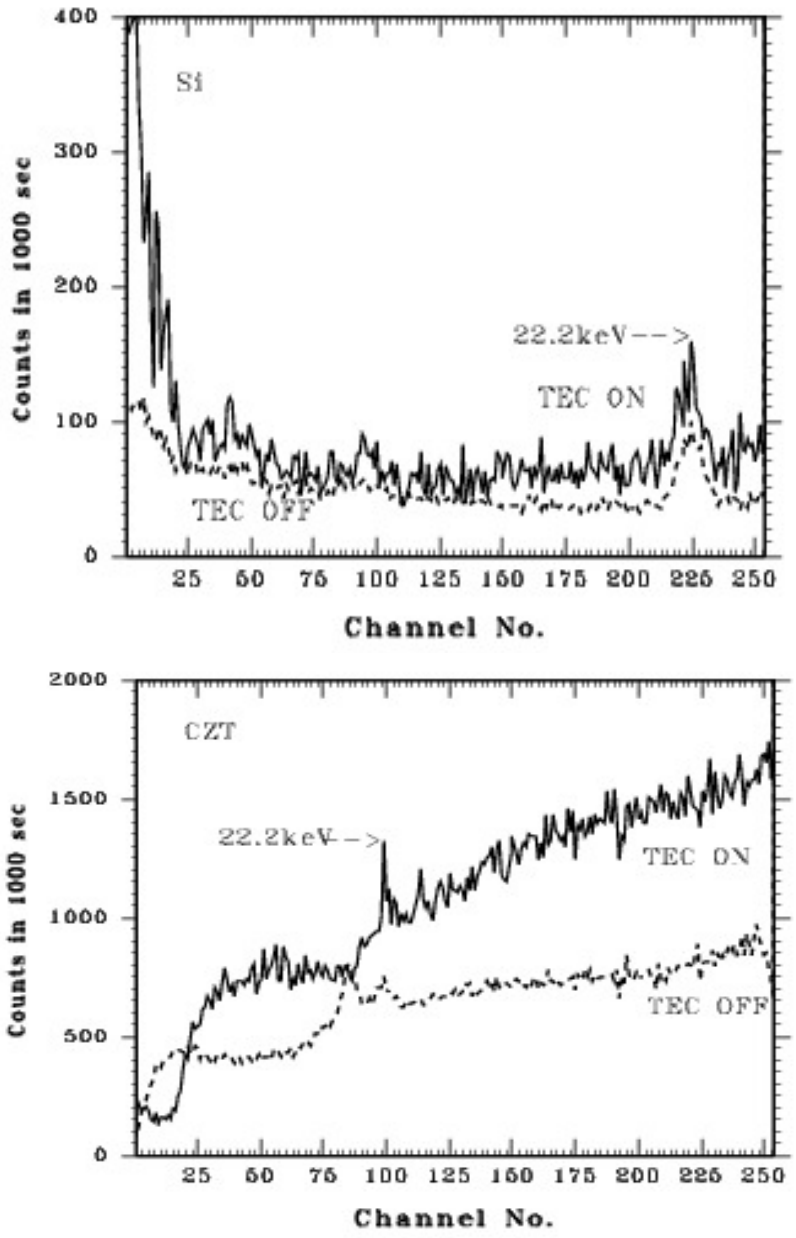

Figure 2.4: In-orbit calibration test with thermoelectric cooler (TEC) ON and OFF, however maintaining the temperature between –15 °C and –25 °C. The 22.2 keV line from onboard radioactive source (mounted inside the collimator) is seen unambiguously in both detectors. However, an anomaly of 14 channel shift in CZT detector may be noticed as soon as TEC is turn ON.

The output flange provides the interface for mounting the main frame. The motor used is SAGEM 35PP 81 04-03-01 redundant winding stepper motor of 1° step angle and the holding torque of 0.6 Nm and drive torque 0.4 Nm. The detailed design specifications may be found in the preliminary design review document prepared by Viswanatha (2000). A Sun sensor is mounted on the

payload (SLED) platform to indicate the Sun axis pointing error during payload operation. The sensor does not operate in a close-loop arrangement. The sensor's FOV is ± 15° and the accuracy is 0.1° in two axes.

2.1.3. Electronics:

2.1.3.1. SLD Front-End Electronics (SFE):

The SLD front-end electronics (SFE) aims to carry out the tasks of pulse shaping, pulse amplification, peak detection, and digital conversion of the input pulse train from the SLED package. In order to achieve these functions the front-end electronics package includes a linear pulse shaping amplifier, peak detectors, 8-bit ADC, energy window discriminators, telemetry interface for house keeping (HK) parameters, and temperature and corona (high voltage) auto-shutoff circuits. It also classifies input energy into nine (four for Si and five for CZT detectors) predefined energy window counters for light curve (temporal mode) observations and flare detection logic. The power supply circuit converts regulated DC voltages from SOXS common electronics (SCE) into required DC voltages for SFE and SLED packages. The package is designed and developed to maintain and reveal detector characteristics *viz.* sub-keV spectral energy resolution and 100 ms temporal resolution

House keeping parameters:

System health is monitored at 1 kHz telemetry rate. 16 house keeping (HK) parameters are monitored at every 16 s through LBT. These parameters provide the information such as detector temperatures, SFE DC-references and salient threshold voltages. Total events recorded in both detectors are also monitored by telemetry.

Detector Protection Circuits:

SFE includes an auto-shut off circuit, which switches off the detector bias voltage as soon as the detector temperature falls out of operating temperature range of −5°C to −30°C so as to protect the detectors from

thermal break down. Corona auto-shut off circuit switches off the detector bias when the bias current increases to 50% above the normal value.

2.1.3.2. SLD Processing Electronics:

SLD processing electronics (SLE) aims to read digital information from the SFE store into onboard memory and upload it to the ground station. The whole data processing electronics are integrated into this package. It consists of 16-bit window counters, ADC interface, real-time pulse height analysis (PHA) circuits for Si and CZT detectors, 5 MB onboard memory to store flare and HK data, on board timer (OBT) and telemetry–telecommand interfaces. This package was designed and developed at Space Astronomy and Instrumentation Division of ISRO Satellite Centre (ISAC), Bangalore (Umapathy *et al.*, 2003). Onboard 16-bit CPU controls all operations of the processing electronics. The SLD current operating mode is programmable via telecommand. SLD has following operating modes:

1. Search, quiet and flare integrated mode.
2. Survey/background mode (100 ms and 1 s).
3. Memory and electronics checkout mode.
4. Readout mode.

Search mode is normal operating mode. In this mode a search is going on for flare onset and quiet phase. Survey mode has been used to study the level of background noise of the quiet Sun. This helps to estimate correct thresholds for flare detection. Memory checkout and read out modes are usable for onboard diagnosis.

2.1.3.3 Flare Triggering Logic:

The SLD operation/observing logic is as follows:

(a) The Survey Mode observes preflare background in the line-of-sight of the Sun and thereby the threshold flux for flare trigger can be determined precisely. However, this default threshold can be modified as and when required through telecommand. This selected threshold flux is equal to 5σ, where σ is measured preflare background during the quiet Sun condition. After completion of Survey Mode during 5–7 June 2003 two default energy windows 10–20 keV for Si and 20–30 keV for CZT detectors were chosen

respectively for flare trigger logic. However, out of nine energy windows any two may be selected for flare detection through telecommand.

(b) As shown in Figure 2.5 during normal observing mode, i.e., Search Mode, the observations in these energy window counters (temporal data) are made always at a cadence of 100 ms but recorded at every 1 s.

(c) The Search Mode will turn into Flare Mode as soon as five consecutive 100 ms observations in any one out of the two energy windows show the flux ≥ threshold that is set in these windows.

(d) The Flare Mode, however, lasts only for 287.5 s, as shown in Figure 2.5, with a temporal resolution of 100 ms for energy windows (temporal) and PHA (spectral). After 287.5 s the logic returns to *Quiet Mode*, which continues for 2274 s and observations are made at a cadence of 1 and 3 s in windows and PHA respectively irrespective of new flare occurrence during this period. This design is carried out in context to limited onboard memory and telemetry rate as well as keeping in mind the most interesting period for high time resolution observations during the flare is first 5 min. After completion of quiet mode the logic returns to search mode automatically. Both Si and CZT detectors are competent to observe soft and hard X-ray micro flares.

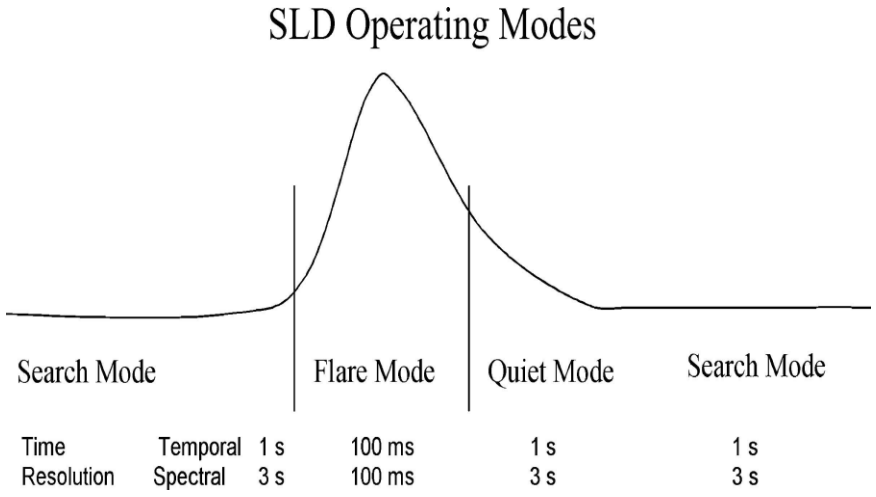

Figure 2.5*:* The operation logic of the SLD payload. The temporal resolution during flare mode is100 ms.

2.1.3.4 SOXS Common Electronics (SCE):

The SOXS common electronics (SCE) is truly common for both low energy and high-energy payloads. SCE package provides common interface to all

SOXS packages with spacecraft (S/C) bus. It minimizes the chance of damage to the mainframe bus because of any anomaly in the packages. SCE consists of low voltage DC/DC converters, high current ART converters, power electronics, telemetry/telecommand interfaces, base-band data encoder, convolution encoder, pre-modulation filter, Sun sensor and SOXS Sun tracking mechanism (SSTM) drive electronics. This package is also designed and developed at Space Astronomy and Instrumentation Division of ISAC, Bangalore (Sharma *et al*., 2000).

2.2 RHESSI:

The Reuven Ramaty High-Energy Solar Spectroscopic Imager (RHESSI) was designed to investigate particle acceleration and energy release in solar flares, through high resolution imaging and spectroscopy of hard X-ray/gamma-ray continua emitted by energetic electrons, and of gamma-ray lines produced by energetic ions. RHESSI was launched in February 2002, into a nearly-circular, 38° inclination, and low-Earth orbit, and began observations a week later. As of today, it continues to successfully operate with similar observing capabilities as at launch. RHESSI is a solar-pointed spinning spacecraft with a nominal rotation period of ~4 sec. The detailed mission overview is provided by Lin *et al*. (2002). I have used the RHESSI Spectrometer observations in chapter 4 and 5. Here, I provide a brief overview of RHESSI spectrometer.

2.2.1 RHESSI Spectrometer – The Germanium detectors:

The RHESSI spectrometer is described in detail by Smith *et al*. (2002). It is composed of nine cryogenically cooled coaxial germanium detectors (GeD). A cutaway of the Spectrometer showing the location of the germanium detectors (by number) is shown in Figure 2.6. When ultra pure germanium is at cryogenic temperatures, no electron-hole pairs are in the conduction band, but a hard X-ray or gamma – ray photon interacting in the crystal will release many energetic electrons, which lose energy by creating free pairs. If there is a high electric field (~1000 V cm^{-1}) across the crystal, the electrons and holes will be pulled to each electrode, creating a current pulse that can be amplified

and digitized by suitable electronics. Figure 2.7 shows a germanium detector. A special arrangement of the electrodes and the field lines allows a single germanium detector to be operated as two segments, a front segment and a rear segment. X-rays (primarily below ~200 keV) have shallow penetration in Ge and are measured primarily in the front segment, while higher-energy gamma rays penetrate more deeply and are measured primarily in the rear segment.

One of the unique features of the RHESSI spectrometer is its high spectral resolution which allows for the accurate measurement of even extremely steep power-law spectra. Energy resolution of the front detectors is about 1 keV (for 3-100 keV). For the rear detectors, it is around 3 keV (for higher energies upto 17 MeV). Photons from 3 keV to 17 MeV can be detected. RHESSI can also detect micro flares in the 3-10 keV range.

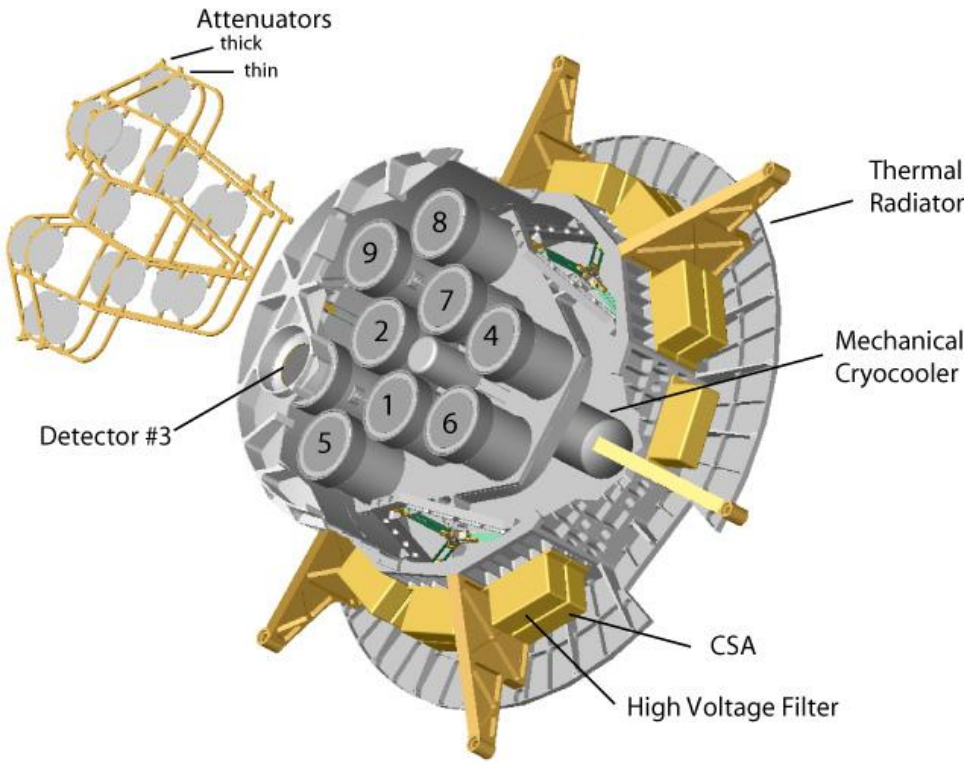

Figure 2.6: A cutaway of the Spectrometer showing the location of the germanium detectors (by number). (Lin *et al*. 2002).

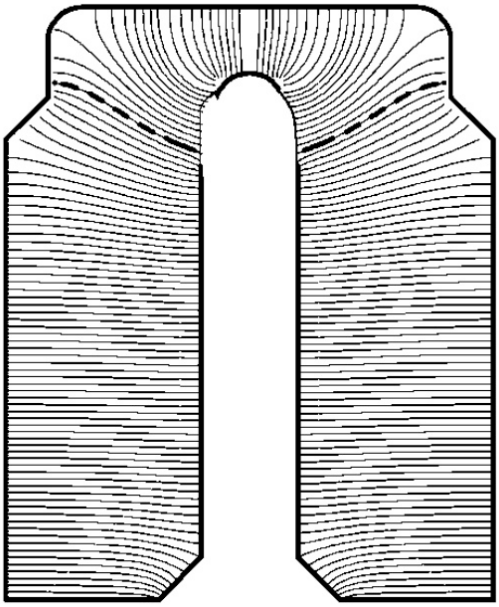

Figure 2.7: Schematic cross-section of one RHESSI germanium detector, showing the electric field lines, with the field line marking the segment boundary in bold dashes (from Smith *et al*. 2002).

Attenuators:

To the top of the spectrometer are two light weight movable frames, each holding nine aluminium discs – thin and thick attenuators – that can be moved in front of the nine GeDs to attenuate the incident SXR flux. Because flare emission is strongly dominated by lower-energy photons, attenuating the SXR flux reduces detector dead time and pulse pileup, maintaining accurate spectroscopy for higher-energy photons above ~ 6 keV even during periods with high incident SXR fluxes. The centers of the attenuators are thinned to preserve some low-energy response – the transmitted flux is reduced by 1/*e* below ~15 and ~25 keV for the thin and thick attenuators, respectively.

Consequently, the detector resolution below ~10 keV is somewhat improved in attenuator states A1 and A3 (to ~0.75 keV FWHM, compared to ~1 keV nominally), as the low-energy photons are then detected only at the center of the GeDs, where the electric fields are strongest, charge travel distance is smallest, and charge collection is fastest. Although all attenuators of a given type (thin or thick) move together, the thin and thick attenuators can be inserted independently. In practice, only three of four modes are used, in order of increasing attenuation: A0 – no attenuators (when both sets of attenuators are held out of the detector lines of sight to the Sun); A1 – thin

attenuators only (when the X-ray counting rate from a flare increases above a prescribed level); and A3 – thin and thick attenuators engaged (if the emission increases still further to another prescribed count rate level). The on-board computer automatically engages the appropriate attenuators as the detector-averaged live time drops below specified thresholds (~92% for A0, ~90% for A1). When the live time remains above 99% for ~4 minutes, the most recent attenuator is disengaged. If the now-unattenuated rates are still sufficiently high so that the live time falls below the threshold, the attenuator is reinserted, and the process repeats; the data during these successive attenuator changes should generally be omitted during spectral analysis.

Background:

The background counts are mainly due to the induced radioactivity of the detectors and due to cosmic ray and trapped particle radiation. The background count rates vary roughly sinusoidally over the orbit of the spacecraft, with the highest rates occurring when RHESSI reaches its highest geomagnetic latitude (~ 50°).

2.2.2 Data handling for Spectral Analysis:

The minimal on-board processing of the photon data maximizes the flexibility for data analysis. Since photons are precisely tagged with the energy they deposit in the germanium detectors and their arrival time, they can be accumulated in arbitrary energy and time bins to produce spectra optimized for the analyst's needs, whether to maximize sensitivity, resolution, statistics, etc. However, because of attenuation, dead time, and various other factors, the observed count spectrum is not identical to the incident photon spectrum, and any analysis must compensate for the effect of the instrument. Much of this is (or can be) done automatically via the RHESSI SSW software (Schwartz *et al*. 2002).

The spectra must also be corrected for count decimation. To prevent the on-board memory from filling too quickly during high count rates, the flight computer employs a progressive decimation scheme whereupon *M* of every *N*

counts below an energy *E* are automatically discarded, with *N* and *E* functions of the memory fill level, attenuator state, and segment (front or rear). Since the decimation scheme is exact, the original count flux can be precisely reconstructed by multiplying the measured count rate below energy *E* by *N/M* (in practice, this can be folded into the live time correction). However, because fewer count rates are observed for the same incident flux, decimation causes an increase in the Poisson noise of the derived count rate.

For a given photon energy, the photo-peak efficiency is the percentage of incident photons that are recorded as counts with that same energy, within the detector resolution; this is represented by the main diagonal of the DRM, and components of the response which affect primarily the photo-peak efficiency are termed “diagonal” components. These include: Grid transmission, Attenuator, blanket, & Be window transmission, Low-level discriminator. In flares, although the photon flux typically rises exponentially with decreasing energy, these three factors combine to yield a photo-peak efficiency that drops even faster; the measured count flux actually decreases below a peak energy (~6 keV for A0, ~10 keV for A1, and ~18 keV for A3), and the counts below this energy become quickly dominated by other than the diagonal response.

Contributions to the response that map an incident photon energy to a different measured count energy further reduce the photo-peak efficiency and are termed “off-diagonal” elements; they include: Energy resolution, K-escape, Compton scattering, Albedo & Pulse pileup. With the exception of those that are functions of the electronics, all of the above response components (specifically: grid transmission, attenuation, K-escape, Compton scattering, and albedo) assume that the incoming photons are incident along the axis, i.e. from the Sun. For such spectral analysis to be accurate and well-defined, the non-solar background must be subtracted from the data before analysis.

2.3 GOES:

In chapter 5, I have employed the proton flux data from the geostationary operational environmental satellites (GOES) Space Environment monitor (SEM). GOES have been developed for National Oceanic and Atmospheric Administration (NOAA) by the National Aeronautics and Space Administration (NASA). The (SEM) measures solar radiation in the X-ray and EUV region and the in-situ magnetic field and energetic particle environment at geosynchronous orbit, providing real-time data to the NOAA Space Weather Prediction Center (SWPC). GOES satellites provide continuous monitoring necessary for intensive data analysis. They circle the Earth in a geosynchronous orbit, which means they orbit the equatorial plane of the Earth at a speed matching the Earth's rotation. The geosynchronous plane is about 35,800 km above the Earth, high enough to allow the satellites a full-disc view of the Earth. The Space Environment Monitor (SEM) subsystem onboard GOES consists of four instruments: An energetic particles sensor (EPS), high energy proton and alpha detector (HEPAD), X-ray sensor (XRS) and two redundant three-axis magnetometers. HEPAD monitors the incident flux density of protons, alpha particles, and electrons over an extensive range of energy levels. XRS monitors the solar output. Two redundant three-axis magnetometers operate one at a time to monitor earth’s geomagnetic field strength in the vicinity of the spacecraft. The SEM instruments are capable of ground command-selectable, in-flight calibration for monitoring on-orbit performance and ensuring proper operation (GOES data book).

Energetic Particles Sensor:

The EPS/ GOES at geostationary orbit performs three integral measurements of electrons from 0.6 to more than 4.0 MeV, a seven-channel differential analysis of protons from 0.8 to 500 MeV, and a six-channel differential analysis of alpha particles from 4 to 500 MeV per nucleon. The EPS also provides all the support required by the HEPAD, which extends the EPS energy ranges to greater than 700 MeV for protons and to greater than 3400 MeV per nucleon for alphas. The EPS and HEPAD are housed within the spacecraft main body and view the space environment through apertures.

The EPS unit consists of a telescope subassembly, a dome subassembly and signal analyzer unit/data processing unit (SAU/DPU); the latter unit provides the final amplification of the telescope and dome output signals. These components are housed on a separate panel, mounted on the spacecraft's south equipment panel, providing a clear field of view towards the west.

The telescope uses two silicon surface barrier detectors that output charge pulses to charge sensitive preamplifiers within the telescope, converting them into voltage pulses; this preconditions the signals sent to the SAU/DPU. These detectors sense low energy protons in the range of 0.8 to 15 MeV and alpha particles in the range of 4 to 60 MeV. The two detectors, surrounded by tungsten shielding, are arranged in a telescope configuration: a 50-μm, 100-mm^2 front detector and a 500-μm, 200-mm^2 rear detector. Tungsten collimators define the field of view of 70° and eliminate detector edge effects. Sweeping magnets exclude electrons below about 100 keV, while a 0.145-mil aluminum foil excludes light. The outer surface of the front solid-state detector is covered with 130 $\mu g/cm^2$ of aluminum, rendering it light tight. The dome employs three sets of two 1500-μm, 25-mm^2, silicon surface barrier detectors, each with different thickness moderators covering the respective pairs' independent fields of view, thus providing three different energy thresholds. As in the telescope, the solid state detector output charge pulses are passed through charge sensitive preamplifiers, converting them into voltage pulses before being routed to the SAU/DPU. After processing, the output of the detector pairs provides data for four proton, three alpha, and three electron energy bands, ranging from 15 to 500 MeV for protons, 60 to 500 MeV for alphas, and less than 0.6 to more than 4.0 MeV for electrons. Table 2.4 shows the energy ranges for the energetic particles sensor.

2.4 SOHO:

SOHO, the Solar and Heliospheric Observatory, is a project of international cooperation between ESA and NASA to study the Sun, from its deep core to the outer corona, and the solar wind. The scientific payload of SOHO

comprises 12 complementary instruments, developed and furnished by 12 international consortia involving 29 institutes from 15 countries. In chapter 5, I have used the Extreme ultraviolet Imaging Telescope (EIT) and Large Angle and Spectrometric Coronagraph (LASCO) observations to establish the flare-CME correlationship and the dynamic and physical properties of CMEs.

2.4.1 SOHO/EIT:

The Extreme-ultraviolet Imaging Telescope (EIT) provides wide-field images of the corona and transition region on the solar disc and up to 1.5 R_s above the solar limb (Delaboudinière *et al*. 1995). Its normal incidence multilayer-coated optics selects spectral emission lines from Fe IX (171 Å), Fe XII (195 Å), Fe XV (284 Å), and He II (304 Å) to provide sensitive temperature diagnostics in the range from 6×10^4 K to 3×10^6 K. The telescope has a 45×45 arcmin field of view and 2.6 arcsec pixels which provides approximately 5-arcsec spatial resolution. The EIT probes the coronal plasma on a global scale, as well as the underlying cooler and turbulent atmosphere, providing the basis for comparative analyses with observations from both the ground and other SOHO instruments.

2.4.2 SOHO/LASCO:

The Large Angle Spectroscopic Coronagraph (LASCO) is a three coronagraph package which has been jointly developed for the Solar and Heliospheric Observatory (SOHO) mission by the Naval Research Laboratory (USA), the Laboratoire d'Astronomie Spatiale (France), the Max-Planck-Institut für Aeronomie (Germany), and the University of Birmingham (UK). LASCO comprises three coronagraphs, C1, C2, and C3, that together image the solar corona from 1.1 to 30 R_s (C1: 1.1- 3 R_s, C2: 1.5-6 R_s, and C3: 3.7 - 30 R_s) (Brueckner *et al*. 1995). The C1 coronagraph is a newly developed mirror version of the classic internally-occulted Lyot coronagraph, while the C2 and C3 coronagraphs are externally occulted instruments. However, only C2 and C3 data are used for uniformity because C1 was disabled in June 1998. A layout of the basic Lyot Coronagraph is shown in Figure 2.8.

Table 2.4 (Energy ranges for the Energetic Particles Sensor)

Particle Type	Channel Designation	Nominal Energy Range (MeV)	Detector Assembly
Proton	P1	≤0.8 to 4	Telescope
Proton	P2	4 to 9	Telescope
Proton	P3	9 to 15	Telescope
Proton	P4	15 to 40	Dome
Proton	P5	40 to 80	Dome
Proton	P6	80 to 165	Dome
Proton	P7	165 to 500	Dome
Proton	P8	350 to 420	HEPAD
Proton	P9	420 to 510	HEPAD
Proton	P10	510 to 700	HEPAD
Proton	P11	> 700	HEPAD
Alpha	A1	4 to 10	Telescope
Alpha	A2	10 to 21	Telescope
Alpha	A3	21 to 60	Telescope
Alpha	A4	60 to 150	Dome
Alpha	A5	150 to 250	Dome
Alpha	A6	300 to 500	Dome
Alpha	A7	2560 to 3400	HEPAD
Alpha	A8	> 3400	HEPAD
Electron	E1	≥ 0.6	Dome
Electron	E2	≥ 2.0	Dome
Electron	E3	≥ 4.0	Dome
“Singles”	S1 to S5	--	HEPAD

Table reproduced from GOES databook.

A solar image is formed by the objective lens O1 at the internal occulter D1. The field lens F1 forms an image of the objective lens onto the Lyot stop A3, where diffracted light from the edge of the lens is prevented from reaching the focal plane. The second objective O2 relays the solar image onto the focal plane.

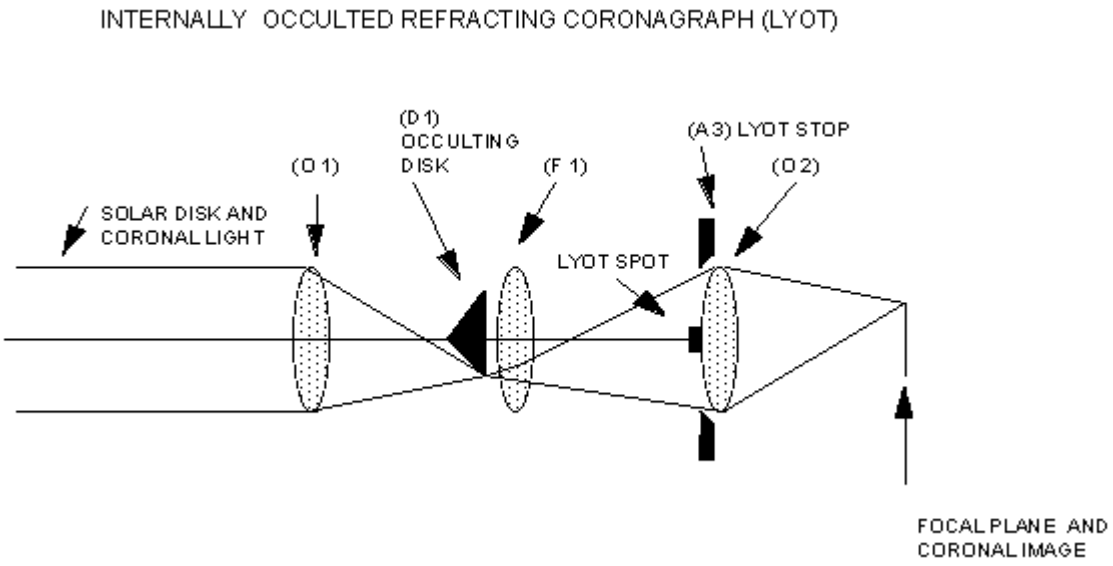

Figure 2.8: Optical components of the Lyot Coronagraph: Objective lens O1, internal occulter D1, Field lens F1, Lyot stop A3, Lyot spot, objective lens O2, and focal plane. (Image: NASA)

B: Ground-based Instruments:

2.5 Magnetic Sensors (Dst Index):

In chapter 5, I have considered the geoeffectiveness in terms of Dst index. The storm-time disturbance index Dst is calculated at the World Data Center WDC at Kyoto, Japan using hourly-mean magnetic observatory data from four standard observatories at low to mid-latitudes (Hermanus, HER; Honolulu, HON; Kakioka, KAK and San Juan, SJG).

The basic sensor package at each observatory consists of a tri-axial fluxgate magnetometer which gathers vectorial data, typically the horizontal intensity, declination, and the vertical component (H, D, Z), plus a proton magnetometer, which measures the total intensity of the field (F). The redundancy between these two measurement systems allows for consistency checks that are useful for troubleshooting. Moreover, a fluxgate sensor-electronics package is prone to deliver data that drift on an absolute scale, primarily as the result of changes in ambient temperature; proton magnetometer data also drift with temperature, but usually much less than fluxgate data. To reduce this baseline drift, the sensors and electronics are housed in well-insulated, thermostatically-controlled buildings, but even then

there remains some residual baseline drift. ‘Absolute’ measurements are made using a theodolite coupled to a small magnetometer; these data are used later during data processing to make final adjustments to the data baselines. To preserve sensor orientation, both the fluxgate magnetometer and the theodolite are supported by piers that are firmly anchored into the ground. This information is acquired from the following website: http://geomag.usgs.gov/operations.php#sensors.

2.6 Magnetic sensors (aa index):

To predict the amplitude of solar cycle 24 (chapter 6), I have used a precursor technique which employs geomagnetic activity index *aa*. The *aa*-index is a simple global geomagnetic activity index. It is derived from the *K* indices from two approximately antipodal observatories and has units of 1 nT. The *aa* index represents the activity level at invariant magnetic latitude of about 50°. The two observatories were Greenwich (1868 – 1925) in the northern hemisphere and Melbourne (1868 – 1919) in the southern hemisphere. Greenwich was replaced by Abinger in 1926 and by Hartland in 1957. Melbourne was substituted by Toolangui in 1920 and by Canberra in 1980. The observatories employ two sets of sensors for magnetic measurements. A tri-axial linear-core fluxgate magnetometer is used to measure the variations in the horizontal (H) and vertical (Z) components of the field. The third sensor is oriented perpendicular to these, and measures variations which are proportional to changes in the declination (D). Measurements are made at a rate of 1 Hz. A proton precession magnetometer (PPM) measures the total intensity of the field (F) at a rate of 0.1 Hz. A fluxgate sensor mounted on a theodolite is used to determine D and inclination (I). (Hartland Observatory, Monthly Magnetic Bulletin, March 2011).

In next Chapter 3 I describe data acquisition and analysis techniques.